



A dilatancy approach to estimating the bearing capacity of shallow foundations on sand  
by Craig Robert Madson

A thesis submitted in partial fulfillment of the requirements for the degree of Master of Science in Civil Engineering

Montana State University

© Copyright by Craig Robert Madson (1996)

Abstract:

Conventional bearing capacity solutions to shallow foundations resting on sand predict that the ultimate bearing capacity increases linearly with footing width and embedment depth. Numerous studies have found this not to be the case. It has been postulated that this observation is due to scale effects arising from non-linear material behavior and progressive failure. The objective of this research was to develop a new design approach to estimate the bearing capacity of sand that 1) accounts for both components of the scale effect and 2) eliminates the need for extensive biaxial testing to establish a material failure envelope. This has been accomplished using dilatancy and strength relationships proposed by Bolton (1986).

In order to evaluate the new approach, results from bearing capacity experiments and shear strength tests were accumulated for 8 study sands. Two of the sands were tested extensively by the author, while data concerning the other 6 sands was collected from previous findings by other researchers. In this thesis, predictions of ultimate bearing capacity using the new approach were compared to the bearing capacity results compiled for each study sand. These predictions were also compared to predictions made using the actual failure envelope of each sand in order to study errors associated with using Bolton's simplified empirical equations.

In general, it was found that using Bolton's empirical equations to estimate the bearing capacity of the study sands did not add an unreasonable amount of error to the predictions. In some cases, using this approach even improved the predictions. These findings are a significant step forward in the estimation of the bearing capacity of sands in that subsurface exploration and material evaluation can be greatly simplified, while at the same time, maintaining reasonable accuracy in bearing capacity predictions.

A DILATANCY APPROACH TO ESTIMATING THE BEARING CAPACITY OF  
SHALLOW FOUNDATIONS ON SAND

by

Craig Robert Madson

A thesis submitted in partial fulfillment  
of the requirements for the degree

of

Master of Science

in

Civil Engineering

MONTANA STATE UNIVERSITY  
Bozeman, Montana

April 1996

N378  
M2673

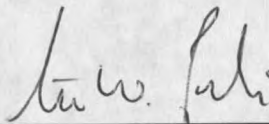
APPROVAL

of a thesis submitted by

Craig Robert Madson

This thesis has been read by each member of the thesis committee and has been found to be satisfactory regarding content, English usage, format, citations, bibliographic style, and consistency, and is ready for submission to the College of Graduate Studies.

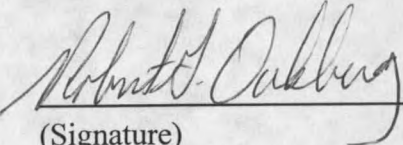
Dr. Steven W. Perkins

  
\_\_\_\_\_  
(Signature)

3-29-96  
Date

Approved for the Department of Civil Engineering

Dr. Robert Oakberg

  
\_\_\_\_\_  
(Signature)

3/29/96  
Date

Approved for the College of Graduate Studies

Dr. Robert Brown

  
\_\_\_\_\_  
(Signature)

4/21/96  
Date

## STATEMENT OF PERMISSION TO USE

In presenting this thesis in partial fulfillment of the requirements for a master's degree at Montana State University-Bozeman, I agree that the Library shall make it available to borrowers under rules of the Library.

If I have indicated my intention to copyright this thesis by including a copyright notice page, copying is allowable for scholarly purposes, consistent with "fair use" as prescribed in the U.S. Copyright law. Requests for permission for extended quotation from or reproduction of this thesis in whole or in parts may be granted only by the copyright holder.

Signature



Date

3/29/96

Dedicated to the memory of Reverend Greg Kaiser

During the course of preparing this thesis, a very old and dear friend by the name of Greg Kaiser died in an unfortunate accident. Words simply cannot convey the respect and admiration held for this man. Greg approached life with a zest that was unparalleled. Whether he was preaching from the pulpit on a Sunday morning, scouting for elk in the mountains, participating in activities with his friends, or simply spending time with his family his devotion was absolute. He gave of himself freely, never asking for anything in return. Greg was dearly loved by all who knew him, and will be sorely missed. It is in his memory that this thesis is dedicated.

## ACKNOWLEDGMENTS

The author would like to express his appreciation to Dr. Steven W. Perkins for his continued guidance and support leading to the completion of this thesis. The author also extends his appreciation to the faculty of the Department of Civil Engineering for their guidance in the academic progress of this student.

Finally, the author would like to express his appreciation to his family and friends for their continued support and patience during the academic career of the author.

## TABLE OF CONTENTS

	Page
1. INTRODUCTION .....	1
Background and Problem .....	1
Scope of Work .....	5
2. LITERATURE REVIEW .....	9
Introduction .....	9
Strength and Dilatancy Behavior of Sands .....	9
Friction Angle .....	9
Dilatancy .....	18
Stress-Dilatancy Theory .....	20
Overview of the General Bearing Capacity Equation .....	27
Methods to account for material non-linearity .....	31
Scale Effects .....	36
3. MATERIAL PROPERTIES OF STUDY SANDS .....	42
Introduction .....	42
Experimental Work .....	43
Grain Size Distributions .....	43
Conventional Triaxial Compression Tests (CTC) .....	44
Centrifuge Bearing Capacity Experiments .....	51
Scaling Relationships .....	52
Experimental Set-up .....	52
Specimen Preparation .....	53
Experimental Results .....	55
Summary of Study Sands .....	59
Toyoura Sand .....	59
Inagi Sand .....	62
Texas Sand .....	65
Ottawa Sand .....	68
Monterey Sand .....	70
Scoria Sand .....	72
Conclusion .....	76
4. DESIGN PROCEDURE FOR BEARING CAPACITY ANALYSIS .....	77
Introduction .....	77
The Bearing Capacity Equation .....	82
Prediction of $q_{ult-peak}$ using Bolton's Equations .....	83
Incorporation of the Index of Progressive Failure ( $I_{PF}$ ) .....	89

Influence of using Bolton's Equations .....	98
Conclusion .....	116
5. SUMMARY, CONCLUSIONS AND RECOMMENDATIONS FOR FURTHER WORK .....	118
Summary .....	118
Conclusions .....	120
Recommendations for Further Study .....	122
REFERENCES CITED .....	124
APPENDICES .....	127
Appendix A Conventional triaxial compression and plane strain test results accumulated for the study sands .....	128
Appendix B Bearing capacity results for the study sands .....	152
Appendix C Comparison of the strength envelopes predicted by Bolton with results from triaxial or plane strain data from each of the study sands ..	165
Appendix D Fortran programs written to solve for the bearing capacity of shallow foundations on sand .....	172

## LIST OF TABLES

	Page
Table 1. Secant friction angles at various levels of $p'$ for MLS-1 & JSC-1 compacted to 100% relative density .....	49
Table 2. Bearing Capacity Results - MLS-1 & JSC-1. ....	58
Table 3. Bearing Capacity Results - Toyoura Sand. ....	60
Table 4. Bearing Capacity Results - Inagi Sand. ....	64
Table 5. Bearing Capacity Results - Texas Sand .....	67
Table 6. Bearing Capacity Results - Ottawa Sand. ....	69
Table 7. Bearing Capacity Results - Monterey Sand. ....	71
Table 8. Physical Properties of Scoria Sand (from Kusakabe et al., 1992). ....	73
Table 9. Bearing Capacity Results - Scoria Sand .....	74
Table 10. Assumed material properties of study sands .....	88
Table 11. Values of $m$ , $\eta$ , and $p_c$ for each sand. ....	99
Table 12. Root mean square (RMS) for each study sand. ....	107

## LIST OF FIGURES

	Page
Figure 1. Modes of failure: (a) general shear, (b) local shear, c) punching shear, (from Craig, 1992). . . . .	3
Figure 2. Analogy of particle interlock. . . . .	12
Figure 3. Interaction of the 3 components of the friction angle. . . . .	14
Figure 4. Friction Angle vs Relative Density for a number of sands (from Hilf, 1975). . . . .	16
Figure 5. Strain conditions under a strip footing. . . . .	17
Figure 6. Typical drained triaxial results for both a dense and loose sand. . . . .	18
Figure 7. Saw blade model of dilatancy. . . . .	21
Figure 8. Stress-dilatancy relations from Bolton (1986). . . . .	23
Figure 9. Ratio of $p'/q_{ult}$ vs $\phi$ (from Perkins, 1995a). . . . .	34
Figure 10. Non-linear dependence of $q_{ult}$ on $B$ , $q$ , or $p$ . . . . .	36
Figure 11. Normalized bearing capacity ( $N\gamma_q$ ) plotted against footing width ( $B$ ) for JSC-1, (from Perkins and Madson, 1996). . . . .	37
Figure 12. Radiograph studies - propagation of shear strains through Toyoura sand at different load steps for small (FG-3) and large (FC-3) scale footings (from Yamaguchi et al., 1976). . . . .	38
Figure 13. Comparison of the scale effect for JSC-1 and Inagi sand (from Perkins and Madson, 1996 and Kusakabe et al., 1991). . . . .	40
Figure 14. Particle Distributions - MLS-1 & JSC-1, (from Perkins and Madson, 1996). . . . .	43
Figure 15. MLS-1 - Peak and residual strength envelopes plotted in $p'$ - $q$ stress space (from specimens compacted to 100% relative density). . . . .	47

Figure 16. MLS-1 - Peak strength envelope plotted in $p'$ - $q$ stress space (from specimens compacted to 61.5% relative density). . . . .	47
Figure 17. MLS-1 - Peak strength envelope plotted in $p'$ - $q$ stress space (from specimens compacted to 28% relative density). . . . .	48
Figure 18. JSC-1 - Peak and residual strength envelopes plotted in $p'$ - $q$ stress space (from specimens compacted to 100% relative density). . . . .	50
Figure 19. MLS-1 - Bearing capacity results; $D = 0$ . . . . .	54
Figure 20. MLS-1 - Bearing capacity results; $D = 0.5B$ . . . . .	54
Figure 21. MLS-1 - Bearing capacity results; $D = 1B$ . . . . .	55
Figure 22. JSC-1 - Bearing capacity results; $D = 0$ . . . . .	57
Figure 23. Toyoura sand - Peak strength envelope plotted in $p'$ - $q$ stress space (from triaxial tests conducted at 34% relative density): . . . . .	61
Figure 24. Toyoura sand - Peak strength envelope plotted in $p'$ - $q$ stress space (from triaxial tests conducted at 75% relative density). . . . .	61
Figure 25. Toyoura sand - Peak strength envelope plotted in $p'$ - $q$ stress space (from plane strain tests conducted at 61% relative density). . . . .	62
Figure 26. Inagi sand - Peak strength envelope plotted in $p'$ - $q$ stress space (from triaxial tests conducted at 80% relative density). . . . .	65
Figure 27. Texas sand - Peak strength envelope plotted in $p'$ - $q$ stress space (from triaxial tests conducted on reconstituted samples at 55% relative density). . . . .	67
Figure 28. Ottawa sand - Peak strength envelope plotted in $p'$ - $q$ stress space (from triaxial tests conducted at 88% relative density). . . . .	70
Figure 29. Monterey sand - Peak strength envelope plotted in $p'$ - $q$ stress space (from triaxial tests conducted at 93% - 95% relative density). . . . .	72
Figure 30. Scoria sand - Peak strength envelope plotted in $p'$ - $q$ stress space (from triaxial tests conducted at approximately 118% relative density). . . . .	75
Figure 31. $I_{PF}$ vs $I_R$ - Developed using Bolton's equations. . . . .	91

Figure 32. $N\gamma_q$ vs $I_R$ - MLS-1 & JSC-1 - Predicted using Bolton's equations. ....	94
Figure 33. $N\gamma_q$ vs $I_R$ - Scoria Sand - Predicted using Bolton's equations. ....	95
Figure 34. $N\gamma_q$ vs $I_R$ - Toyoura Sand - Predicted using Bolton's equations. ....	95
Figure 35. $N\gamma_q$ vs $I_R$ - Inagi Sand - Predicted using Bolton's equations. ....	96
Figure 36. $N\gamma_q$ vs $I_R$ - Monterey Sand - Predicted using Bolton's equations. ....	96
Figure 37. $N\gamma_q$ vs $I_R$ - Texas Sand - Predicted using Bolton's equations. ....	97
Figure 38. $N\gamma_q$ vs $I_R$ - Ottawa Sand - Predicted using Bolton's equations. ....	97
Figure 39. $I_{PF}$ vs $I_R$ - Developed using the actual $p'$ - $q$ strength envelope. ....	101
Figure 40. $N\gamma_q$ vs $I_R$ - MLS-1 & JSC-1- Predicted using $p'$ - $q$ strength envelopes. ...	103
Figure 41. $N\gamma_q$ vs $I_R$ - Scoria Sand - Predicted using $p'$ - $q$ strength envelope. ....	104
Figure 42. $N\gamma_q$ vs $I_R$ - Toyoura Sand - Predicted using $p'$ - $q$ strength envelope. ....	104
Figure 43. $N\gamma_q$ vs $I_R$ - Inagi Sand - Predicted using $p'$ - $q$ strength envelope. ....	105
Figure 44. $N\gamma_q$ vs $I_R$ - Monterey Sand - Predicted using $p'$ - $q$ strength envelope. ....	105
Figure 45. $N\gamma_q$ vs $I_R$ - Texas Sand - Predicted using $p'$ - $q$ strength envelope. ....	106
Figure 46. $N\gamma_q$ vs $I_R$ - Ottawa Sand - Predicted using $p'$ - $q$ strength envelope. ....	106
Figure 47. Amount of over/under pred. with MLS-1 & JSC-1 using Bolton's equations. ....	108
Figure 48. Amount of over/under pred. with MLS-1 & JSC-1 using $p'$ - $q$ strength envelope. ....	108
Figure 49. Amount of over/under pred. with Scoria sand using Bolton's equations. ....	109
Figure 50. Amount of over/under pred. with Scoria sand using $p'$ - $q$ strength envelope. ....	109

Figure 51. Amount of over/under pred. with Toyoura sand using Bolton's equations. ....	110
Figure 52. Amount of over/under pred. with Toyoura sand using $p^{\prime}$ - $q$ strength envelope. ....	110
Figure 53. Amount of over/under pred. with Inagi sand using Bolton's equations. ....	111
Figure 54. Amount of over/under pred. with Inagi sand using $p^{\prime}$ - $q$ strength envelope. ....	111
Figure 55. Amount of over/under pred. with Monterey sand using Bolton's equations. ....	112
Figure 56. Amount of over/under pred. with Monterey sand using $p^{\prime}$ - $q$ strength envelope. ....	112
Figure 57. Amount of over/under pred. with Texas sand using Bolton's equations. ....	113
Figure 58. Amount of over/under pred. with Texas sand using $p^{\prime}$ - $q$ strength envelope. ....	113
Figure 59. Amount of over/under pred. with Ottawa sand using Bolton's equations. ....	114
Figure 60. Amount of over/under pred. with Ottawa sand using $p^{\prime}$ - $q$ strength envelope. ....	114
Figure 61. MLS-1 CTC results at 100% relative density, (from Perkins and Madson, 1996). . . . .	129
Figure 62. MLS-1 CTC results at $\sigma'_3 = 6.89, 3.44, \text{ and } 1.72 \text{ kPa}$ ; 61.5% relative density, (from Perkins, 1991). . . . .	130
Figure 63. MLS-1 CTC results at $\sigma'_3 = 13.8 \text{ kPa}$ ; 61.5% relative density (from Perkins, 1991). . . . .	131
Figure 64. MLS-1 CTC results at $\sigma'_3 = 34.4 \text{ kPa}$ ; 61.5% relative density (from Perkins, 1991). . . . .	132

Figure 65. MLS-1 CTC results at $\sigma'_3 = 68.9$ kPa; 61.5% relative density (from Perkins, 1991). . . . .	133
Figure 66. MLS-1 CTC results at $\sigma'_3 = 6.89, 3.44,$ and $1.72$ kPa; 28% relative density, (from Perkins, 1991). . . . .	134
Figure 67. MLS-1 CTC results at $\sigma'_3 = 13.8$ kPa; 28% relative density (from Perkins, 1991). . . . .	135
Figure 68. MLS-1 CTC results at $\sigma'_3 = 34.4$ kPa; 28% relative density (from Perkins, 1991). . . . .	136
Figure 69. MLS-1 CTC results at $\sigma'_3 = 68.9$ kPa; 28% relative density (from Perkins, 1991). . . . .	137
Figure 70. JSC-1 CTC results at 100% relative density, (from Perkins and Madson, 1996). . . . .	138
Figure 71. Toyoura sand shear strength data from CTC tests, (from Fukushima and Tatsuoka, 1984). . . . .	139
Figure 72. Toyoura sand shear strength data from plane strain tests; 61% relative density, (from Tatsuoka et al., 1986). . . . .	139
Figure 73. Inagi sand CTC results; approximately 80% relative density (from Kusakabe et al., 1991). . . . .	140
Figure 74. Change in angle of shearing resistance with relative density for Inagi sand (from Kusakabe et al., 1991). . . . .	140
Figure 75. Texas sand - CTC results for samples taken at 0.6 m; approximately 55% relative density (from Briaud and Gibbens, 1994). . . . .	141
Figure 76. Texas sand - CTC results for samples taken at 3.0 m; approximately 55% relative density (from Briaud and Gibbens, 1994). . . . .	141
Figure 77. Ottawa sand - CTC results at approximately 88% relative density (from Aiban, 1991). . . . .	142
Figure 78. Ottawa sand CTC results at $\sigma'_3 = 1.72$ kPa; approximately 88% relative density, (from Schipporeit, 1988). . . . .	143

Figure 79. Ottawa sand CTC results at $\sigma'_3 = 5.17$ kPa; approximately 88% relative density, (from Schipporeit, 1988). . . . .	144
Figure 80. Ottawa sand CTC results at $\sigma'_3 = 34.48$ kPa; approximately 88% relative density, (from Schipporeit, 1988). . . . .	145
Figure 81. Ottawa sand CTC results at $\sigma'_3 = 103.43$ kPa; approximately 88% relative density, (from Schipporeit, 1988). . . . .	146
Figure 82. Variation in the peak friction angle with mean normal stress for Monterey sand; approximately 93-95% relative density, (from Kutter et al., 1988). . . . .	147
Figure 83. Monterey sand CTC results at $\sigma'_3 = 21$ kPa; approximately 93-95% relative density, (from Abghari, 1987). . . . .	148
Figure 84. Monterey sand CTC results at $\sigma'_3 = 53$ kPa; approximately 93-95% relative density, (from Abghari, 1987). . . . .	148
Figure 85. Monterey sand CTC results at $\sigma'_3 = 100$ kPa; approximately 93-95% relative density, (from Abghari, 1987). . . . .	149
Figure 86. Monterey sand CTC results at $\sigma'_3 = 200$ kPa; approximately 93-95% relative density, (from Abghari, 1987). . . . .	149
Figure 87. Monterey sand CTC results at $\sigma'_3 = 400$ kPa; approximately 93-95% relative density, (from Abghari, 1987). . . . .	150
Figure 88. Monterey sand CTC results at $\sigma'_3 = 690$ kPa; approximately 93-95% relative density, (from Abghari, 1987). . . . .	150
Figure 89. Scoria sand CTC results; approximately 118% relative density (from Kusakabe et al., 1992). . . . .	151
Figure 90. Mohr's circles at failure for Scoria sand; approximately 118% relative density, (from Kusakabe et al., 1992). . . . .	151
Figure 91. Relationship between $N\gamma_q$ and $\gamma B_N/E_q$ for Toyoura sand (from Kimura, 1995). . . . .	153
Figure 92. Toyoura sand bearing capacity results for a) $B = 3$ cm; $D/B = 0$ b) $B = 120$ cm; $D/B = 0$ , (from Kimura, 1995). . . . .	153

Figure 93. Toyoura sand bearing capacity results for a)  $B = 3$  cm;  $D/B = 0.5$   
 b)  $B = 120$  cm;  $D/B = 0.5$ , (from Kimura, 1995). . . . . 154

Figure 94. Toyoura sand bearing capacity results for a)  $B = 80$  cm;  $D/B = 1.0$   
 b)  $B = 120$  cm;  $D/B = 1.0$ , (from Kimura, 1995). . . . . 154

Figure 95. Toyoura sand bearing capacity results for a)  $B = 160$  cm;  $D/B = 1.0$   
 (from Kimura, 1995). . . . . 155

Figure 96. Toyoura sand bearing capacity results for a)  $B = 3$  cm;  $D/B = 1.0$   
 b)  $B = 4$  cm;  $D/B = 1.0$ , (from Kimura, 1995). . . . . 155

Figure 97. Inagi sand bearing capacity results for a)  $L/B = 1$  b)  $L/B = 3$ ,  
 (from Kusakabe et al., 1991). . . . . 156

Figure 98. Inagi sand bearing capacity results for an  $L/B = 7$   
 (from Kusakabe et al., 1991).. . . . . 156

Figure 99. Texas sand bearing capacity results for 3.004 x 3.004 m footing;  
 $D/B = 0.25$ , (from Briaud and Gibbens, 1994). . . . . 157

Figure 100. Texas sand bearing capacity results for 1.505 x 1.492 m footing;  
 $D/B = 0.51$ , (from Briaud and Gibbens, 1994). . . . . 158

Figure 101. Texas sand bearing capacity results for 3.023 x 3.016 m footing;  
 $D/B = 0.29$  (from Briaud and Gibbens, 1994). . . . . 159

Figure 102. Texas sand bearing capacity results for 2.489 x 2.496 m footing;  
 $D/B = 0.31$ , (from Briaud and Gibbens, 1994). . . . . 160

Figure 103. Texas sand bearing capacity results for 0.991 x 0.991 m footing;  
 $D/B = 0.72$ , (from Briaud and Gibbens, 1994). . . . . 161

Figure 104. Ottawa sand bearing capacity results for 1.14 m footing;  
 $D/B$  from 0 to 1, (from Aiban, 1991). . . . . 162

Figure 105. Monterey sand bearing capacity results for circular footings;  
 $D/B = 0$ , (from Kutter et al., 1988). . . . . 163

Figure 106. Scoria sand bearing capacity results, (from Kusakabe et al., 1992). . . . . 164

Figure 107. MLS-1- comparison of Bolton's prediction of the strength envelope and  
 the strength envelope developed from CTC results (100% relative density). . . 166

- Figure 108. MLS-1 - comparison of Bolton's prediction of the strength envelope and the strength envelope developed from CTC results (61.5% relative density). . 166
- Figure 109. MLS-1- comparison of Bolton's prediction of the strength envelope and the strength envelope developed from CTC results (28% relative density). . . . 167
- Figure 110. JSC-1 - comparison of Bolton's prediction of the strength envelope and the strength envelope developed from CTC results. . . . . 167
- Figure 111. Scoria sand - comparison of Bolton's prediction of the strength envelope and the strength envelope developed from CTC results. . . . . 168
- Figure 112. Toyoura sand - comparison of Bolton's prediction of the strength envelope and the strength envelope developed from CTC results (74.5% rel. density). . 168
- Figure 113. Toyoura sand - comparison of Bolton's prediction of the strength envelope and the strength envelope developed from CTC results (34.1% rel. density). . 169
- Figure 114. Toyoura sand - comparison of Bolton's prediction of the strength envelope and the strength envelope developed from plane strain tests (61% relative density). . . . . 169
- Figure 115. Inagi sand - comparison of Bolton's prediction of the strength envelope and the strength envelope developed from CTC results. . . . . 170
- Figure 116. Monterey sand - comparison of Bolton's prediction of the strength envelope and the strength envelope developed from CTC results. . . . . 170
- Figure 117. Texas sand - comparison of Bolton's prediction of the strength envelope and the strength envelope developed from CTC results. . . . . 171
- Figure 118. Ottawa sand - comparison of Bolton's prediction of the strength envelope and the strength envelope developed from CTC results. . . . . 171

## ABSTRACT

Conventional bearing capacity solutions to shallow foundations resting on sand predict that the ultimate bearing capacity increases linearly with footing width and embedment depth. Numerous studies have found this not to be the case. It has been postulated that this observation is due to scale effects arising from non-linear material behavior and progressive failure. The objective of this research was to develop a new design approach to estimate the bearing capacity of sand that 1) accounts for both components of the scale effect and 2) eliminates the need for extensive triaxial testing to establish a material failure envelope. This has been accomplished using dilatancy and strength relationships proposed by Bolton (1986).

In order to evaluate the new approach, results from bearing capacity experiments and shear strength tests were accumulated for 8 study sands. Two of the sands were tested extensively by the author, while data concerning the other 6 sands was collected from previous findings by other researchers. In this thesis, predictions of ultimate bearing capacity using the new approach were compared to the bearing capacity results compiled for each study sand. These predictions were also compared to predictions made using the actual failure envelope of each sand in order to study errors associated with using Bolton's simplified empirical equations.

In general, it was found that using Bolton's empirical equations to estimate the bearing capacity of the study sands did not add an unreasonable amount of error to the predictions. In some cases, using this approach even improved the predictions. These findings are a significant step forward in the estimation of the bearing capacity of sands in that subsurface exploration and material evaluation can be greatly simplified, while at the same time, maintaining reasonable accuracy in bearing capacity predictions.

## CHAPTER 1

### INTRODUCTION

#### Background and Problem

In the course of performing a structural design, adequate consideration must be given to the basic support system of the structure, namely, the foundation system. The primary purpose of the foundation is simply to transmit loads to the underlying soil structure. Transmittal of these loads may be done through the use of either footings or rafts. Footings are slabs which provide support to a portion of the structure. Individual footings are often used to support single columns. Footings used to support groups of columns are referred to as combined footings, while load-bearing walls are supported with the use of strip footings. In contrast, a raft footing is a large single slab supporting the entire structure. In cases where the upper layers of soil are incapable of providing sufficient support, piles or drilled piers are often used to transmit the structural loads to suitable soils found at greater depths.

In this thesis, the discussion will be limited to the design of shallow foundations placed on sand. We will not be looking at the design of piles or drilled piers. Perhaps at this point it would be helpful to define the meaning of a shallow foundation. Foundations are considered shallow if the depth, ( $D_f$ ) of the footing is less than or equal to 3 - 4 times the width (B).

In general, a shallow foundation must meet two requirements. First, any settlement induced by the foundation must be within an acceptable limit. In other words, settlement of the foundation should not cause unacceptable damage or, in anyway, interfere with the basic function of the structure. Secondly, the foundation should be designed in such a manner as not to exceed the ultimate bearing capacity ( $q_{ult}$ ) of the soil. Here, we are mainly concerned with the possibility of general shear failure resulting in catastrophic damage to the structure. It should be noted that one of these two requirements will often control the design of a foundation. For example, the bearing capacity of the soil may be sufficient to support the structure, yet the settlement associated with the load may be excessive. Therefore, the importance of the function of the structure will play a major role in determining which criteria will control.

Throughout the remainder of this thesis, we will be limiting the discussion to making accurate predictions of bearing capacity, while ignoring any settlement requirements. More specifically, we will be looking at a new technique to make better predictions of the bearing capacity of sands.

In order to better understand discussions throughout the remainder of this thesis, it would perhaps be insightful to provide a definition of the ultimate bearing capacity ( $q_{ult}$ ). Craig (1992) defines  $q_{ult}$  as "the least pressure which would cause shear failure of the supporting soil immediately below and adjacent to a foundation". In general, failure may occur by one of three modes (see Figure 1). General shear failure is associated with the development of a failure surface extending to ground level. Often, general shear failure is accompanied with upheaval of the ground surface immediately adjacent to the structure. In

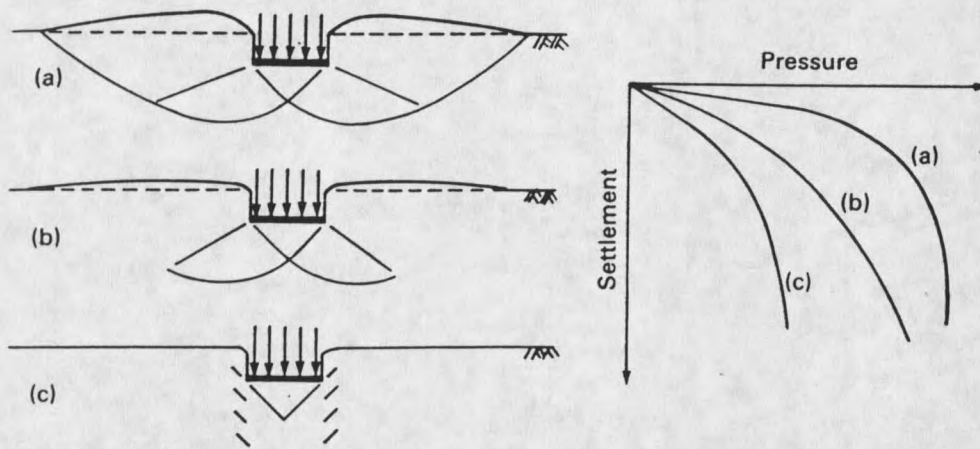


**Figure 1.** Modes of failure: (a) general shear, (b) local shear, c) punching shear, (from Craig, 1992).

this mode, the ultimate bearing capacity is normally well defined as seen in Figure 1. Failures such as this often occur within dense or stiff soils. In contrast, local shear failure is often associated with only a partial development of a failure surface. Unlike the previous mode, considerable displacement must occur for the failure surface to reach ground surface. The last mode of failure, punching failure, occurs in loose or soft soils and at increased depths of embedment. In this mode, the failure surface does not extend to the ground surface, and the ultimate bearing capacity is often not clearly defined as may be seen in Figure 1. In general, it may be said that the final 2 modes of failure are often associated with excessive settlements of the foundation that ultimately control the design. In contrast, general shear failure is often the failure mode in cases where the ultimate bearing capacity is controlling the design.

In light of the above discussion, the engineer is now left with the problem of making accurate predictions of ultimate bearing capacity in cases where bearing capacity controls.

While conventional solutions exist for bearing capacity problems, in the past, these solutions have been applied with some inherent conservatism, (i.e., relatively large factors of safety). This often may be attributed to the nonhomogeneous conditions that can be found at a particular site. However, in some cases, this conservatism is due to a failure to appreciate the intricacies of soil-structure interaction. Specifically, the following are often not understood.

(a) that a fundamental relationship exists between the dilatancy and strength of a soil, and that the rate of dilation, which is dependent upon the effective stress and density, can be related to appropriate strength parameters. Dilatancy may be defined as the volumetric increase associated with the shearing of a dense sand.

(b) that the scale effect composed of material non-linearity and progressive failure will lower expected bearing capacities, especially at higher mean normal stress levels beneath the footing.

Conventional solutions to bearing capacity problems predict that the ultimate bearing capacity will increase linearly with footing width and embedment depth, and fail to consider scale effects composed of material non-linearity and progressive failure observed in bearing capacity experiments. Material non-linearity may be thought of as the dependence of the peak friction angle on the mean normal stress level ( $p'$ ) beneath the footing. Higher levels of mean normal stress corresponding to increased footing widths and embedment depths are associated with lower peak friction angles. Since conventional solutions assume that the friction angle remains constant with increasing  $p'$ , they will often over predict the actual bearing capacity at increased footing widths and embedment depths. The second component of the scale effect, progressive failure, is due to the nonuniform distribution of shear strain and thus peak shear resistance along the slip surface. Peak strength has already been reached

and exceeded in regions close to the footing, long before the shear strength in regions further away has been mobilized. As a result, the average angle of shearing resistance is decreased and the ultimate bearing capacity is lowered. Radiograph studies by Yamaguchi et al., (1976) indicate that this becomes a greater problem with increasing size and embedment depth of the footing, (i.e., increasing  $p'$ ). Conventional solutions assume that uniform peak shear resistance is occurring along the entire slip surface.

### Scope of Work

The objective of this thesis will be to present a dilatancy approach to the design of vertically loaded shallow foundations resting on sand. Eccentric loadings of shallow foundations are not considered. This approach utilizes dilatancy and strength relationships developed by Bolton (1986). The design methodology separately accounts for both material non-linearity and progressive failure and, at the same time, eliminates the need for extensive shear strength testing in order to define a material failure envelope. In order to evaluate the new design procedure, bearing capacity predictions were compared to results accumulated from bearing capacity experiments performed on 8 study sands. Additionally, predictions made using Bolton's equations were compared to predictions made using the failure envelope of each study sand.

The previous section described, in general terms, the idea of ultimate bearing capacity, and defined some of the problems associated with attempting to evaluate bearing capacity using conventional methods. This section will provide an overview of the different aspects of the study, as well as a brief description of the layout of this thesis.

As noted above, the newly proposed approach to the design of shallow foundations was evaluated using bearing capacity data and shear strength data accumulated for 8 study sands. In all, 61 bearing capacity experiments were used. Bearing capacity tests included both full-scale tests and model experiments using the centrifuge. Shear strength tests included triaxial and plane strain tests. The author performed triaxial tests on two of the study sands (MLS-1 and JSC-1), in conjunction with centrifuge tests performed on these sands by previous researchers. Bearing capacity and shear strength data on the other 6 study sands was accumulated from a variety of sources including papers, research journals, and theses. In some cases, the authors were contacted to acquire further information regarding their research.

The bearing capacity data was analyzed and tabulated for each study sand. Information recorded for each experiment included both the density and relative density of the sand tested, the size and embedment depth of the footing, and the corresponding ultimate bearing capacity. The type of test (full-scale or centrifuge) was also noted in this study, as well as any other experimental factors such as the presence of a groundwater table. In several cases, the load displacement curves demonstrated strain hardening characteristics, (i.e., no peak load). Therefore, the peak load had to be chosen to correspond to a particular normalized settlement ( $S/B$ ) of the footing, where  $S$  and  $B$  are the settlement and footing width, respectively.

Shear strength data provided with each study sand was also evaluated by the author. Using the data, peak strength envelopes were developed in  $p'$ - $q$  stress space for each study sand. This was done for two reasons. First, Bolton's equations use empirical constants to

describe the strength characteristics of a particular sand. The error associated with using these empirical constants was studied by comparing the strength envelope they predict, with the strength envelope developed for each study sand. Second, bearing capacity predictions using the proposed method were compared to predictions using the actual peak strength envelope. This necessitated the development of a peak strength envelope for each study sand. The strength data was also analyzed to find an appropriate constant volume friction angle ( $\phi'_{cv}$ ) for each sand. The constant volume friction angle is simply the friction angle associated with the critical state, (i.e., the point at which shearing takes place without any change in volume). As will be shown in later chapters, the constant volume friction angle is primarily dependent upon the mineralogy of the sand. Bolton's relationships incorporate the use of the constant volume friction angle, and for this reason, an appropriate constant volume friction angle had to be chosen for each study sand.

In order to use Bolton's equations, the level of mean normal stress ( $p'$ ) appropriate to the footing has to be found. This required the development of an expression relating the mean normal stress ( $p'$ ) and resulting ultimate bearing capacity ( $q_{ult}$ ), to an appropriate friction angle. Perkins (1995a) demonstrated that the ratio of mean normal stress to ultimate bearing capacity ( $p'/q_{ult}$ ) is primarily a function of the friction angle ( $\phi'$ ). Using a non-linear limit plasticity solution, an expression was found that related  $p'/q_{ult}$  to  $\phi'$ . This equation is given in Chapter 4.

The next chapter of this thesis will begin with an overview of the behavior of sands. This chapter includes an in-depth discussion of the friction angle, including factors that will influence the friction angle of a given sand. Dilatancy characteristics of sand will also be

presented, followed by a brief discussion of stress-dilatancy theory by Rowe (1962). Rowe's theories lay the groundwork for Bolton's empirical equations relating dilatancy and strength of sand presented later in the chapter. Also discussed will be several analytical solutions proposed by other researchers to bearing capacity problems on sand. The last section of the chapter will be devoted to a presentation of the scale effect, composed of material non-linearity and progressive failure. The scale effect has been noted by numerous researchers and was briefly described earlier.

Chapter 3 will present the experimental work performed by the author on two of the study sands (MLS-1 and JSC-1). In addition, material properties, bearing capacity results, and shear strength data for the other 6 study sands will be given. Included within this section will be a brief narrative on the testing procedure used in performing bearing capacity and shear strength experiments on each of the study sands.

Chapter 4 presents a detailed description of the proposed design procedure for estimating the bearing capacity of sands. This procedure will separately account for material non-linearity and progressive failure, and will utilize dilatancy-strength relationships proposed by Bolton (1986). The predictions made using Bolton's equations will be compared to the bearing capacity results, as well as to predictions made using the actual strength envelope of each sand.

The last chapter will be devoted to conclusions and recommendations for further work. Also discussed will be simple tests that may be used to establish the material parameters required in Bolton's equations.

## CHAPTER 2

### LITERATURE REVIEW

#### Introduction

The literature review in this chapter consists of three sections: strength and dilatancy behavior of sands, overview of the general bearing capacity equation, and a discussion of scale effects which influence the response of shallow foundations.

In section one, the strength and dilatancy properties of sands are discussed in detail. This section provides much of the background required to study the bearing capacity problem. Section two discusses several approaches used to solve bearing capacity problems. These approaches form the basis for the analysis techniques discussed in Chapter 4. The last section presents a discussion of scale effects composed of material non-linearity and progressive failure, and observed in shallow foundation experiments.

#### Strength and Dilatancy Behavior of Sands

##### Friction Angle

The resistance of a soil to shear is governed by the soil's shear strength. In order to solve soil stability problems such as bearing capacity problems, a knowledge of the shear strength parameters is required. Coulomb originally expressed the shear strength at failure

$(\tau_f)$  as a linear function of the normal stress ( $\sigma_f$ ).

$$\tau_f = c + \sigma_f \tan \phi \quad (1)$$

This equation is known as the Mohr-Coloumb failure criteria, and is more properly expressed as a function of effective normal stress as

$$\tau_f = c' + \sigma_f' \tan \phi' \quad (2)$$

where  $c'$  and  $\phi'$  are shear strength parameters describing the effective cohesion intercept and the effective angle of shearing resistance or friction angle. Failure of a soil mass will therefore occur on a particular plane at any point where a critical combination of effective normal and shear stress develops.

In practice, the cohesion term in granular soils such as sands is often assumed to be zero resulting in the simplified Mohr-Coloumb failure criteria presented as

$$\tau_f = \sigma_f' \tan \phi' \quad (3)$$

where the shear strength of the sand is simply expressed as a function of  $\phi'$ .

The friction angle of a sand is normally considered to consist of three components.

These components are:

1. Mineral to mineral sliding or grain sliding ( $\phi_u$ )
2. Particle interlocking, dilation (geometric effect) ( $\theta$ )
3. Rolling friction ( $\phi_r$ )

Rowe (1962) found that the grain sliding component ( $\phi_u$ ) is generally dependent upon several variables including:

- (1) Mineral Composition
- (2) Microscopic surface roughness
- (3) Testing technique
- (4) Particle size
- (5) Surface conditions

$\phi_u$  has, in reality, been shown to be principally a function of mineralogy. For example, the grain sliding component ( $\phi_u$ ) of feldspar, a common mineral found in sands, can be as high as 37 degrees, while silica quartz sands have been found to be as low as 26 degrees, (Mitchell, 1976).

The second component of the friction angle (particle interlocking) is associated with the work required to lift particles over one another leading to volume expansion or dilation of the sample. This component may be better understood by consideration of Figure 2.

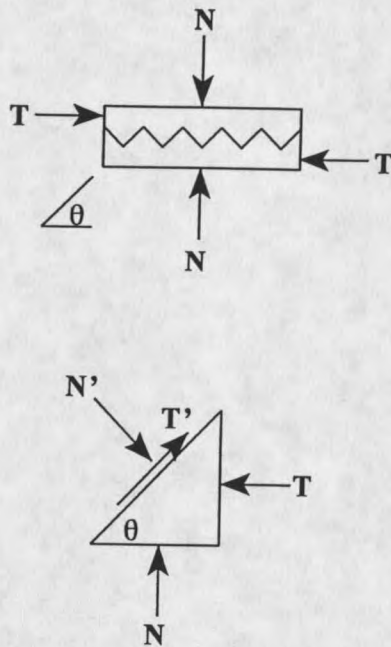


**Figure 2.** Analogy of particle interlock.

By requiring static equilibrium, the following expressions may be developed:

$$T' = T \cos \theta - N \sin \theta \quad (4)$$

$$N' = T \sin \theta - N \cos \theta \quad (5)$$

The law of friction can be used to relate  $N'$  to  $T'$  by

$$T' = N' \tan \phi_u \quad (6)$$











































































































































































































































































































































